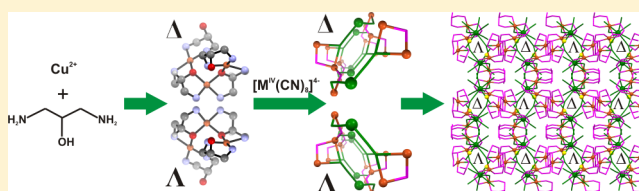


Chiral $(\text{LH})_2\text{L}_2\text{Cu}_3$ Trinuclear Paramagnetic Nodes in Octacyanidometalate-Bridged Helical ChainsOlaf Stefańczyk,^{†,‡,§} Michał Rams,^{||} Anna M. Majcher,^{||} Corine Mathonière,^{‡,§} and Barbara Sieklucka^{*,†}[†]Faculty of Chemistry, Jagiellonian University, Ingardena 3, 30-060 Kraków, Poland[‡]CNRS, ICMCB, UPR 9048, F-33600 Pessac, France[§]Univ. of Bordeaux, ICMCB, UPR 9048, F-33600 Pessac, France^{||}Institute of Physics, Jagiellonian University, Reymonta 4, 30-059 Kraków, Poland

Supporting Information

ABSTRACT: Trinuclear chiral $(\text{LH})_2\text{L}_2\text{Cu}_3$ (LH = 1,3-diamino-2-propanol, bdapH) assemblies linked by octacyanidometalate(IV) form isostructural one-dimensional (1D) chains consisting of right- and left-handed helices arranged in an alternate manner: $[(\text{bdapH})_2(\text{bdap})_2\text{Cu}_3] \cdot [\text{M}^{\text{IV}}(\text{CN})_8] \cdot \text{H}_2\text{O}$ (M = Mo 1, W 2). Each chain displays helicity with a long pitch around 17.2 Å. The direction of the helix rotation is strictly connected with the conformation of the $(\text{LH})_2\text{L}_2\text{Cu}_3$ unit. Right-handed helices are based on Δ -S,S- $(\text{LH})_2\text{L}_2\text{Cu}_3$, whereas left-handed ones contain Λ -R,R- $(\text{LH})_2\text{L}_2\text{Cu}_3$ units. Magnetic studies reveal antiferromagnetic interactions through alkoxo-bridges inside trinuclear Cu(II) nodes leading to an $S_T = 1/2$ ground state for both assemblies.



INTRODUCTION

The design and synthesis of chiral magnetic materials combining magnetism and optical activity is one of the major challenges in the pursuit of polyfunctional materials. In this field, extensive research is related to cyanido-bridged coordination polymers based on octacyanidometalates, which exhibit coexistence of chirality with a broad range of magnetic properties, including long-range magnetic ordering,¹ magnetic anisotropy,² and photomagnetism.³ Since the chirality of the compounds must be controlled in the molecular structure, as well as in the entire crystal structure, the access to chiral cyanido-based magnets is not trivial. The reported synthetic strategies comprise programmed coordination of chiral ligands to 3d/4f metal centers, followed by self-assembly with octacyanidometalates^{1b,d,h,2a,4} and serendipitous formation of noncentrosymmetric networks employing achiral ligands.^{1a,c,e-g,i,2b,3,5}

To the best of our knowledge, the only example of the chiral helical system obtained from a chiral ligand is the 1D chain $\{[\text{Eu}^{\text{III}}(\text{R,R/S,S-Pr}^i\text{-Pybox})(\text{dmf})_4]_3[\text{W}^{\text{V}}(\text{CN})_8]_3\}_n \cdot \text{dmf} \cdot 8\text{H}_2\text{O}$ ($\text{Pr}^i\text{-Pybox} = 2,2'-(2,6\text{-pyridinediyl})\text{bis}(4\text{-isopropyl-2-oxazoline})$, dmf = dimethylformamide).⁴ The majority of helical bimetallic magnetic systems based on $[\text{M}(\text{CN})_8]^{4-}$ building blocks were generated from achiral ligands, such as polyamines, polyimines, Schiff bases, and macrocycles.^{3c,5b,d,j,6} Generally, they crystallize in centrosymmetric space groups due to self-assembly of right- (Δ) and left-handed (Λ) helices in an alternate manner. However, spontaneous chiral resolution was reported for $[\text{Ln}^{\text{III}}(\text{dmf})_6][\text{Mo}^{\text{V}}(\text{CN})_8]$ ($\text{Ln}^{\text{III}} = \text{Pr}, \text{Nd}$),^{5b} $[\text{Ni}^{\text{II}}(\text{tren})]_3[\text{Mo}^{\text{IV}}(\text{CN})_8](\text{ClO}_4)_2 \cdot 5\text{H}_2\text{O}$ ($\text{tren} = \text{tris}(2\text{-aminoethyl})\text{amine}$),^{5d} and $[\text{Cu}^{\text{II}}(\text{tren})][\text{Cu}^{\text{II}}(\text{bapa})][\text{Mo}^{\text{IV}}(\text{CN})_8]$.

$4\text{H}_2\text{O}$ (bapa = bis(3-aminopropyl)amine).^{3c} Additionally, in the Cu(II)-Mo(IV) systems, a photomagnetic effect was observed.⁷

In this context, we decided to obtain novel magnetic materials based on chiral polynuclear magnetic Cu(II)-aminoalcohol assemblies. Copper(II) ions with aminoalcohols (L) form numerous polynuclear alkoxo-bridged Cu_xL_y ($2 \leq x \leq 6$, $y \geq x$) systems ensuring strong magnetic coupling.⁸ In particular, Cu(II) complexes with aminoalcohols, such as H_3Tea (triethanolamine) and Hea (ethanolamine), have proven to be successful building blocks for the self-assembly of octacyanidometalate-based coordination polymers.⁹ $[\text{Cu}^{\text{II}}_2(\text{H}_2\text{Tea})_2]_5[\text{W}^{\text{V}}(\text{CN})_8][\text{W}^{\text{IV}}(\text{CN})_8] \cdot x\text{H}_2\text{O}$ and $[\text{Cu}^{\text{II}}(\text{ea})]_4 \cdot [\text{M}^{\text{IV}}(\text{CN})_8] \cdot 2\text{H}_2\text{O}$ (M = Mo, W) are structurally characterized as 3D networks based on alkoxo-bridged dimers $(\text{Cu}_2\text{L}_2) \cdot [\text{Cu}_2(\text{H}_2\text{Tea})_2]^{2+}$ and cubes $(\text{Cu}_4\text{L}_4) \cdot [\text{Cu}(\text{ea})]_4^{4+}$, linked by $[\text{M}(\text{CN})_8]^{4-/3-}$ ions. The assembly built from Cu_2L_2 dimers exhibits antiferromagnetic ordering below 2.2 K, whereas compounds with the Cu_4L_4 units behave like high-spin molecules with $S = 2$ bridged by diamagnetic octacyanidometalate(IV) ions.

Herein, we focus our interest on the unexplored trinuclear $[(\text{bdapH})_2(\text{bdap})_2\text{Cu}_3]^{4+}$ compound revealing an ability to form Δ and Λ spiral structures. The coordination of 1,3-diamino-2-propanol (bdapH) to Cu(II) leads to triangular (L_3Cu_3) ¹⁰ and spiral $((\text{LH})_2\text{L}_2\text{Cu}_3)$ ¹¹ trinuclear complexes (Figure 1). The steric hindrance between terminal bdapH ligands in spiral $(\text{LH})_2\text{L}_2\text{Cu}_3$ units induces chirality on two

Received: February 3, 2014

Published: March 27, 2014

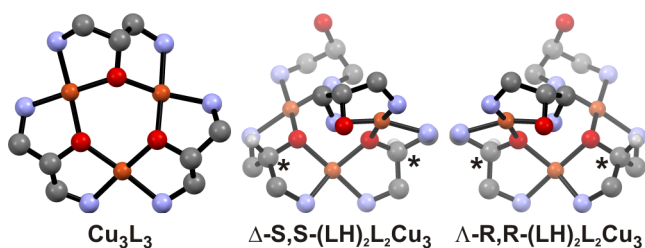


Figure 1. Various structural motifs of trinuclear Cu(II) complexes with bdapH. Hydrogen atoms bounded to chiral carbon are only shown. Colors used: Cu, orange; O, red; N, blue; C, black; H, white.^{10,11}

carbon atoms located on bridging bdap molecules. Hence, the spiral $(LH)_2L_2Cu_3$ unit consists of the right-handed (Δ) form of S,S configurations on chiral carbon atoms, and the left-handed (Λ) form of R,R configurations in the two enantiomeric forms. To the best of our knowledge, the spiral form of $(LH)_2L_2Cu_3$ has never been applied in the synthesis of coordination polymers. Therefore, we decided to connect the trinuclear moiety with octacyanidometalates(IV) with the expectation that novel magnetic properties would be added to those found in the Cu(II)-Mo(IV) systems.⁷ As a result, we obtained 1D helical chains of $[(bdapH)_2(bdap)_2Cu^{II}]_3[M^{IV}(CN)_8] \cdot H_2O$ ($M = Mo$ **1**, **W** **2**) that are the very first examples of a polynuclear chiral building block presence in octacyanidometalate-based systems. Structural, spectroscopic, and magnetic properties are reported and discussed.

EXPERIMENTAL SECTION

Materials. All starting materials were commercially available, reagent grade, and used as purchased without further purification. Potassium octacyanidotungstate(IV) and octacyanidomolybdate(IV) salts have been prepared according to the published procedures.¹² The $[(bdapH)_2(bdap)_2Cu^{II}]_3I_4 \cdot CH_3OH$ ($(LH)_2L_2Cu_3I_4$), as a reference compound for magnetic measurements, has been synthesized according to the published procedure (Supporting Information, Experimental Section).^{11b}

Physical Techniques. Infrared spectra were recorded in KBr pellets in the range of $4000\text{--}400\text{ cm}^{-1}$ using a Bruker EQUINOX 55 FT-IR spectrometer. Elemental analyses (C, H, N) were carried out with an Elementary Vario Micro Cube CHNS. Diffuse reflectance spectra were recorded with a PerkinElmer Lambda 35 UV/vis spectrophotometer equipped with a PerkinElmer Labsphere RSA-PE-20 Reflectance Spectroscopy Accessory and converted with a Kubelka–Munk function. Magnetic measurements on polycrystalline samples were performed using a Quantum Design MPMS XL-5 SQUID magnetometer. All experimental magnetic data were corrected for the diamagnetism of the sample holders and of the constituent atoms (Pascal's tables). Photomagnetic studies were performed on a powdered sample of **1** placed as a thin layer between two transparent films (around 3 mg). Experiments were done with 405, 450, 660, and 843 nm laser diodes, and with 473 and 532 nm diode-pumped solid-state lasers ($P = 25\text{ mW/cm}^2$) coupled through an optical fiber directed into the magnetometer cavity. Experimental data were corrected for sample holder and diamagnetic contribution of the samples using experimentally determined values.

Caution! We did not encounter any problems during our studies; nevertheless, the perchlorate salt compounds are potentially explosive and should be handled with care.

Table 1. Crystal Data, Data Collection, and Refinement Parameters for **1** and **2**

	1	2
molecular formula	$C_{20}H_{40}Cu_3MoN_{16}O_5$	$C_{20}H_{40}Cu_3N_{16}O_5W$
M_r	871.27	959.17
T (K)	120(2)	120(2)
radical used, λ (Å)	Mo $K\alpha$ (0.71073)	Mo $K\alpha$ (0.71069)
cryst syst, space group	orthorhombic, $Pbca$	orthorhombic, $Pbca$
a (Å)	17.2322(5)	17.2460(2)
b (Å)	17.4969(5)	17.5290(2)
c (Å)	20.5736(6)	20.6140(4)
α (deg)	90	90
β (deg)	90	90
γ (deg)	90	90
V (Å ³)	6203.1(3)	6231.72(16)
Z , d_{calc} (g·cm ⁻³)	8, 1.866	8, 2.045
μ (mm ⁻¹)	2.485	5.760
$F(000)$	3528	3784
θ range for data collection (deg)	2.31–36.41	4.77–27.48
index ranges	$-28 \leq h \leq 27$ $-29 \leq k \leq 28$ $-34 \leq l \leq 33$	$-22 \leq h \leq 22$ $-22 \leq k \leq 22$ $-26 \leq l \leq 26$
reflns collected/unique	98 312/15 128 [$R(\text{int}) = 0.0662$]	13 556/7101 [$R(\text{int}) = 0.0140$]
completeness of θ (%)	99.9 ($\theta = 36.41^\circ$)	99.3 ($\theta = 27.48^\circ$)
max/min transmission	0.780/0.627	0.562/0.329
refinement method	full-matrix least-squares on F^2	full-matrix least-squares on F^2
data/restraints/parameters	15 128/0/566	7101/0/562
goodness-of-fit on F^2	0.932	1.083
final R indices ($I > 2\sigma(I)$)	$R_1 = 0.0286$, $wR_2 = 0.0600$	$R_1 = 0.0237$, $wR_2 = 0.0595$
R indices (all data)	$R_1 = 0.0497$, $wR_2 = 0.0634$	$R_1 = 0.0263$, $wR_2 = 0.0613$
largest diff. peak and hole (e ⁻ ·Å ⁻³)	1.480 and -1.136	1.780 and -1.686

Table 2. Selected Bond Lengths (Å) and Angles (deg) for 1 and 2

	bond lengths (Å)				
	1	2	1	2	
M1–C1	2.170(1)	2.179(3)	Cu2–N2	2.289(1)	2.298(3)
M1–C2	2.155(2)	2.162(3)	Cu2–N25	1.995(1)	1.998(2)
C1–N1	1.154(2)	1.150(4)	Cu2–N31	1.992(1)	1.990(3)
C2–N2	1.152(2)	1.152(4)	Cu2–O2	2.001(1)	2.003(2)
Cu1–N1	2.330(1)	2.339(2)	Cu2–O3	1.955(1)	1.959(2)
Cu1–N11	2.021(2)	2.025(3)	Cu3–N2	2.559(1)	2.567(3)
Cu1–N15	1.985(1)	1.988(2)	Cu3–N35	2.004(1)	2.004(3)
Cu1–N21	2.005(2)	2.008(3)	Cu3–N41	2.029(1)	2.030(3)
Cu1–O2	1.980(1)	1.984(2)	Cu3–N45	1.986(1)	1.990(2)
			Cu3–O3	1.989(1)	1.993(2)
	angles (deg)				
	1	2	1	2	
M1–C1–N1	176.60(13)	176.4(2)	C2–N2–Cu3	131.2(1)	131.4(2)
M1–C2–N2	178.25(14)	178.2(2)	Cu1–O2–Cu2	128.61(6)	128.53(10)
C1–N1–Cu1	137.72(12)	137.8(2)	Cu2–O3–Cu3	109.09(5)	109.13(9)
C2–N2–Cu2	142.27(13)	142.2(2)	Cu2–N2–Cu3	82.81(4)	82.68(8)

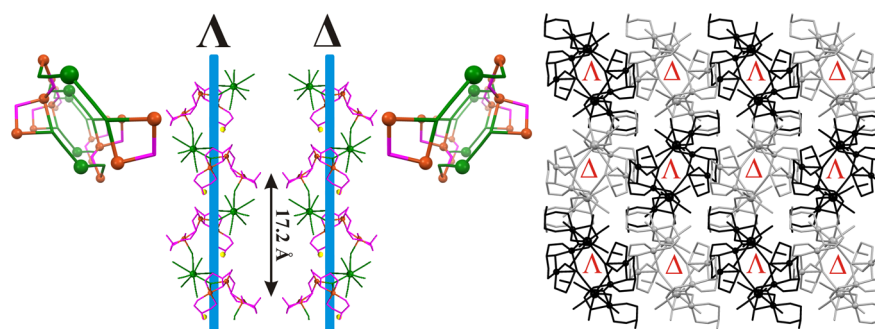


Figure 2. Left: the 1D left- (Λ) and right-handed (Δ) helical chains of 1 and 2. Colors used: [M(CN)₈]⁴⁻, green; Cu²⁺, orange; bdapH, magenta; and water, yellow. Right: crystal packing along *a* axis. Colors used: left-handed helix (Λ), black; right-handed helix (Δ), light gray.

[(bdapH)₂(bdap)₂Cu^{II}]₃[Mo^{IV}(CN)₈]₃·H₂O (1). To the aqueous solution (16 mL) containing Cu(ClO₄)₂·6H₂O (37 mg, 0.1 mmol) and 1,3-diamino-2-propanol (45 mg, 0.5 mmol) was added K₄[Mo(CN)₈]₂·2H₂O (25 mg, 0.05 mmol, 4 mL of H₂O) slowly upon vigorous stirring. The dark blue solution was left undisturbed for slow evaporation in a dark place. Navy blue crystals of 1 were obtained after a few weeks. The product was filtrated, washed with water, and dried in air. Yield of 1: 21.8 mg (75% based on Cu). Elementary Anal. Calcd. for C₂₀H₄₀Cu₃MoN₁₆O₅ (871.21 g/mol): C, 27.57; H, 4.63; N, 25.72%; found: C, 27.36; H, 4.67; N, 25.64%. IR of 1 (KBr, cm⁻¹): 3462s(br), 3303vs(br) [ν(O–H), ν(N–H)]; 3125m, 2924m, 2880w, 2851m [ν(C–H)]; 2124vs, 2109m, 2096vs, 2083vs [ν(C≡N)]; 1600s, 1574s [γ(O–H)]; 1452m, 1413w, 1385w, 1353w, 1330w, 1307m, 1285w, 1219w [δ(H–C–H), ν(N–C), ν(C–C)]; 1187m, 1151w, 1086m, 1049s, 1027s, 962m, 931w, 893w, 847m, 803s, 731s, 635w [γ(N–H out-of-plane), ν(N–C)]; 537m, 505m [ν(Mo–C), ν(Cu–N)]. Solid-state UV–vis–NIR of 1 (nm): 256, 369 [MLCT band of [Mo(CN)₈]⁴⁻]; 430 [MMCT band in Cu(II)–Mo(IV) pair]; 710, 823 [d–d bands of (LH)₂L₂Cu₃] (Supporting Information, Figure S4).

[(bdapH)₂(bdap)₂Cu^{II}]₃[W^{IV}(CN)₈] (2). An analogous procedure to that of 1 was applied, but K₄[W(CN)₈]₂·2H₂O (29 mg, 0.05 mmol) instead of K₄[Mo(CN)₈]₂·2H₂O was used. Yield of 2: 20.5 mg (64% based on Cu). Elementary Anal. Calcd. for C₂₀H₄₀Cu₃N₁₆O₅W (959.11 g/mol): C, 25.05; H, 4.20; N, 23.37%; found: C, 24.93; H, 4.40; N, 23.44%. IR of 2 (KBr, cm⁻¹): 3473s(br), 3303vs(br) [ν(O–H), ν(N–H)]; 3127m, 2924m, 2880w, 2851m [ν(C–H)]; 2124vs, 2110m, 2091vs, 2074vs [ν(C≡N)]; 1600s, 1574s [γ(O–H)]; 1454m, 1412w, 1384w, 1352w, 1331w, 1308m, 1284w, 1220w [δ(H–C–H), ν(N–C), ν(C–C)]; 1186m, 1150w, 1085m, 1047s, 1028s, 961m,

930w, 895w, 845m, 800s, 731s, 634w [γ(N–H out-of-plane), ν(N–C)]; 538m, 483m [ν(W–C), ν(Cu–N)]. Solid-state UV–vis–NIR of 2 (nm): 250, 277, 370 [MLCT band of [Mo(CN)₈]⁴⁻]; 433 [MMCT band in Cu(II)–W(IV) pair]; 710, 831 [d–d bands of (LH)₂L₂Cu₃] (Supporting Information, Figure S4).

X-ray Crystallography. The single-crystal X-ray diffraction measurements were performed with a Bruker APEX II 4476 diffractometer for 1, and a Nonius KappaCCD diffractometer for 2, operating at 50 kV and 30 mA using graphite monochromated molybdenum radiation [$\lambda(\text{Mo } K\alpha) = 0.71073 \text{ \AA}$]. Data collection and reduction were performed using BRUKER SUIT (APEX II) and Denzo and Scalepack (KappaCCD) programs. The structure was solved by direct methods using the package WinGX^{13a} (SIR-97;^{13b} SHELXL-97^{13c}) and refined by *F*² full-matrix refinement. The non-H atoms were refined anisotropically using weighted full-matrix least-squares on *F*². All hydrogen atoms joined to carbon and nitrogen atoms of the organic component of 1 and 2 were positioned with an idealized geometry and refined using a riding model. Hydrogen atoms of crystallization water molecules are unreachable, so their positions were calculated with the XHYDEX program^{13d} or manually at positions optimized to form the hydrogen bonds and refined using a riding model. Crystal data, data collection, and refinement parameters for 1 and 2 are listed in Table 1, and selected bond lengths and bond angles are listed in Table 2. CCDC 978521–978522 contain the supplementary crystallographic data for this paper. These data can be obtained free of charge from The Cambridge Crystallographic Data Centre via www.ccdc.cam.ac.uk/data_request/cif. The structural data presented as figures are prepared with the use of the CCDC Mercury visualization software.^{13e} Geometries of metal centers are estimated

with the Continuous Shape Measures (CShM) analysis with the use of SHAPE v2.0 software (Supporting Information, Tables S1 and S2).^{13f}

RESULTS AND DISCUSSION

Crystal Structure of 1 and 2. Single-crystal X-ray diffraction studies reveal that **1** and **2** are isomorphous, and they form structures containing 1D right- (Δ) and left-handed (Λ) helices arranged in an alternate manner (Figure 2). Each chain is built of $[(\text{bdapH})_2(\text{bdap})_2\text{Cu}_3]^{4+}$ trinuclear units bridged by $[\text{M}(\text{CN})_8]^{4-}$ ions of triangular dodecahedron (TDD-8) geometry (Supporting Information, Figure S1, Table S1).^{13f} Interestingly, each chain displays helicity with a long pitch around 17.2 Å for **1** and **2**. The direction of the helix rotation is strictly connected with the conformation of the $(\text{LH})_2\text{L}_2\text{Cu}_3$ unit. Right-handed helices are based on Δ -S,S- $(\text{LH})_2\text{L}_2\text{Cu}_3$, whereas left-handed ones contain Λ -R,R- $(\text{LH})_2\text{L}_2\text{Cu}_3$ units. This observation leads to the conclusion that chirality is transferred from structural entities to helical chains.¹⁴ The octacyanidometalate(IV) anion forms one cyanido-bridge (C1–N1) to the Cu1 center and one μ_3 -cyanido-bridge (C2–N2) to the Cu2 and Cu3 centers (Supporting Information, Figure S2). An analogous bridging mode was observed for $(\text{LH})_2\text{L}_2\text{Cu}_3$ assemblies with NO_2^- and SCN^- ions.^{11a,c} Average M–C and C–N bond distances in M–C–N–Cu linkages are 2.166 and 1.152 Å, respectively, while M–C–N angles are almost 180°. Each copper(II) center reveals a different 5-coordinate geometry: square-pyramidal (SPY-5) for Cu1, trigonal-bipyramidal (TBPY-5) for Cu2, and intermediate between square-pyramidal (SPY-5) and vacant octahedral (vOC-5) for Cu3 (Supporting Information, Table S2).^{13f} The equatorial positions in terminal $[\text{Cu}(\text{NC})(\text{bdapH})(\text{bdap})]$ units for Cu1 and Cu3 centers are occupied by two nitrogen atoms of chelating bdapH and one nitrogen and one oxygen atom of bridging bdap with an average Cu–L distance of 2.001 Å, while the axial one is occupied by nitrogen of the cyanido-bridge with Cu–N bond lengths in the range of 2.330(1)–2.567(3) Å. In the case of the central $[\text{Cu}(\text{NC})(\text{bdap})_2]$ moiety for Cu2 center, equatorial positions are occupied by oxygen and nitrogen atoms of two different bridging bdap ligands and a nitrogen atom of CN^- , while the axial ones are coordinated by oxygen and nitrogen of bdap bridges with an average Cu2–L distance of 2.048 Å. All CN^- bridges are strongly bent, revealing Cu–N–C angles ranging between 137.72(12)° and 142.27(13)°. In structures of **1** and **2**, long μ_3 -cyanido-bridges with CuX–N distances ranging from 2.2892(14) to 2.567(3) Å and Cu2–N2–Cu3 angles of 82.81(4)° and 82.68(8)° for **1** and **2**, respectively, are present. For both compounds, the Cu1–O–Cu2 and Cu2–O–Cu3 angles are about 128.6° and 109.1°, respectively, whereas the analogous angles for $(\text{LH})_2\text{L}_2\text{Cu}_3\text{I}_4$ are 118.2° and 114.4°.^{13f} The average Cu–O bond length in the μ -alkoxo-bridges in **1** and **2** of 1.983 Å conforms to those reported previously for $(\text{LH})_2\text{L}_2\text{Cu}_3\text{I}_4$. Additionally, the hydrogen-bonding network stabilizes the structure due to interactions between bdapH ligands, water molecules, and nitrogen atoms of terminal CN^- (Supporting Information, Figure S3).

Magnetic Properties. The magnetic properties of polycrystalline samples of **1** and **2** were investigated by measuring the thermal dependence of the molar magnetic susceptibility χ_M in the temperature range of 1.8–300 K and at a magnetic field of 1 kOe. The results in the form of the $\chi_M T$ product per $\text{Cu}_3\text{L}_4\text{M}^{\text{IV}}$ unit versus temperature are shown in Figure 3. The data for **1** and **2** have been compared to the

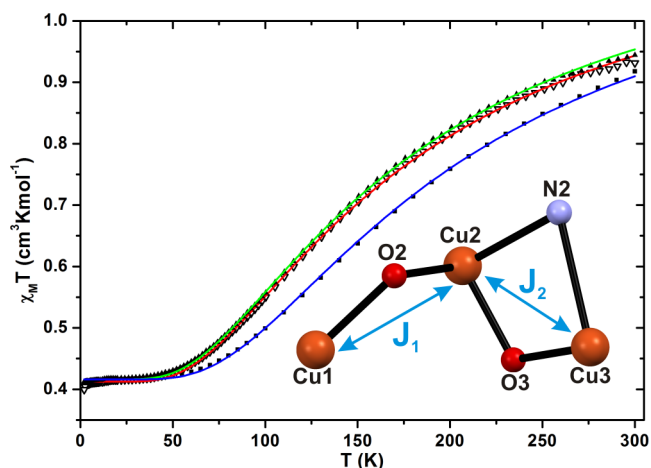


Figure 3. Product of magnetic susceptibility and temperature ($H_{dc} = 1$ kOe) for **1** (empty triangles), **2** (filled triangles), and the reference compound $(\text{LH})_2\text{L}_2\text{Cu}_3\text{I}_4$ (squares). The solid lines correspond to the best theoretical fits (see text) for **1** (red), **2** (green), and for $(\text{LH})_2\text{L}_2\text{Cu}_3\text{I}_4$ (blue). Inset: Scheme of magnetic interactions in **1** and **2**.

magnetic properties of the molecular complex $(\text{LH})_2\text{L}_2\text{Cu}_3\text{I}_4$. The $\chi_M T$ values at 300 K reach 0.93, 0.94, and 0.92 $\text{cm}^3 \text{K mol}^{-1}$ for **1**, **2**, and $(\text{LH})_2\text{L}_2\text{Cu}_3\text{I}_4$, respectively, which are much lower than the expected Curie constant value of 1.13 $\text{cm}^3 \text{K mol}^{-1}$ for three noninteracting spins $S_{\text{Cu}} = 1/2$ with $g = 2.0$. At low temperatures, $\chi_M T$ curves decrease to reach 0.40, 0.41, and 0.40 $\text{cm}^3 \text{K mol}^{-1}$ at 1.8 K for **1**, **2**, and $(\text{LH})_2\text{L}_2\text{Cu}_3\text{I}_4$, respectively. These values are consistent with the Curie constant for a ground state of $S_T = 1/2$, indicating antiferromagnetic coupling inside the $(\text{LH})_2\text{L}_2\text{Cu}_3$ assemblies. The field dependencies of magnetization for **1**, **2**, and $(\text{LH})_2\text{L}_2\text{Cu}_3\text{I}_4$ confirm these observations (Figure 4). The saturation magnetization in a magnetic field of 50 kOe reached values around 1.0 $N\beta$ for all compounds. Fits of the Brillouin function to the experimental data with $S_T = 1/2$ give g values equal 2.06(1), 2.08(1), and 2.08(1) for **1**, **2**, and $(\text{LH})_2\text{L}_2\text{Cu}_3\text{I}_4$, respectively.

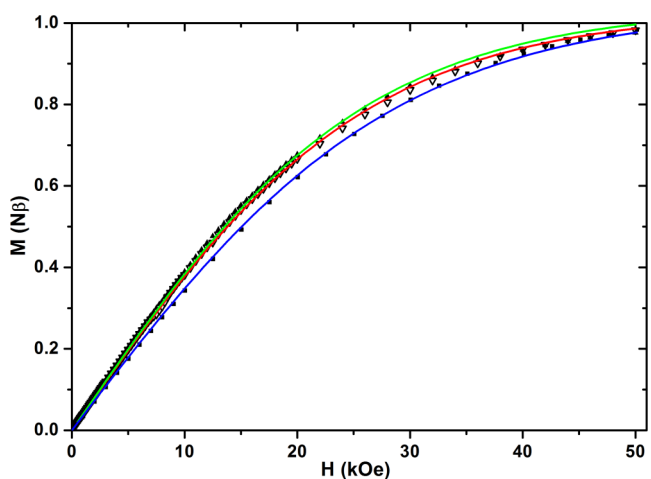


Figure 4. The M vs H plots for **1** (empty triangles) and **2** (filled triangles) measured at 1.8 K and for $(\text{LH})_2\text{L}_2\text{Cu}_3\text{I}_4$ measured at 2 K (squares). The solid lines correspond to Brillouin function fit ($S_T = 1/2$) of **1** (red), **2** (green), and $(\text{LH})_2\text{L}_2\text{Cu}_3\text{I}_4$ (blue).

On the basis of the structural analysis, thermal dependencies of the susceptibility were analyzed in the terms of trinuclear systems defined by the following Hamiltonian: $H = -2J_1S_1S_2 - 2J_2S_2S_3$ assuming Heisenberg exchange interactions between adjacent Cu^{II} centers (Figure 3). From this Hamiltonian, the $\chi_M T$ product of the trimer is calculated as¹⁵

$$\chi_M T = \frac{N_A \mu_B^2 g^2}{4k} \frac{1 + \exp(-\Delta_1/kT) + 10 \exp(-\Delta_2/kT)}{1 + \exp(-\Delta_1/kT) + 2 \exp(-\Delta_2/kT)}$$

$$\text{with } \Delta_1 = -2\sqrt{J_1^2 + J_2^2} - J_1J_2 \text{ and } \Delta_2 = \frac{\Delta_1}{2} - (J_1 + J_2)$$

where N_A is Avogadro's number, μ_B is the Bohr magneton, and k is the Boltzmann constant.

An attempt to fit this model to the experimental data for **1** leads to two different solutions: the first $J_1 = -110(11)$ K, $J_2 = -90(13)$ K, and the second $J_1 = J_2 = -100$ K, with a large fitting error. The qualities of both fits are almost the same. Such ambiguity is a result of overparametrization of the experimental data. It is also not possible to distinguish which J value corresponds to which of the two different Cu–O–Cu bridges. The analysis of the data for **2** leads to similar results. Therefore, a simplest model was used with the additional assumption of $J_1 = J_2 = J$. The average values obtained are: $J = -100(2)$ K, $g = 2.09(1)$ for **1**; $J = -100(2)$ K, $g = 2.10(1)$ for **2**; and $J = -118(1)$ K, $g = 2.11(1)$ for (LH)₂L₂Cu₃I₄. The obtained J value for (LH)₂L₂Cu₃I₄ agrees well with the previously reported results.^{13f} The magnetic properties of **1**, **2**, and (LH)₂L₂Cu₃I₄ are dominated by the strong antiferromagnetic coupling through the alkoxo bridges whose geometry leads to a significant overlap between the magnetic orbitals.

The possible existence of the photomagnetic effect in **1** was thoroughly investigated. The measurements were performed at 10 K, with an applied field of 10 kOe using the following wavelengths of irradiation lines: 405, 450, 473, 532, 660, and 843 nm at $P = 25$ mW/cm², each irradiation lasting 1 h. These particular wavelengths were chosen based on the UV–vis–NIR characteristics of **1** (Supporting Information, Figure S4). No photomagnetic effect for **1** was observed in the experimental conditions employed (Supporting Information, Figure S5).

CONCLUSIONS

As a part of our studies aimed at the synthesis of coordination polymers containing chiral building blocks and octacyanido-metalates, we report two novel 1D helical chains [(bdapH)₂(bdap)₂Cu^{II}₃][M^{IV}(CN)₈].H₂O (M = Mo **1**, W **2**). The spiral intrinsically chiral (bdapH)₂(bdap)₂Cu^{II}₃ trinuclear nodes transfer chirality from the trinuclear nodes to the helical chains. To the best of our knowledge, the helical chains [(bdapH)₂(bdap)₂Cu^{II}₃][M^{IV}(CN)₈].H₂O are the first examples of the presence of polynuclear chiral building blocks in octacyanido-metalate-based systems. Magnetic studies of **1**, **2**, and previously reported [(bdapH)₂(bdap)₂Cu^{II}₃]₄.CH₃OH ((LH)₂L₂Cu₃I₄) reveal antiferromagnetic interactions inside the (bdapH)₂(bdap)₂Cu^{II}₃ units with J values equal to $-100(2)$, $-100(2)$, and $-118(1)$ K for **1**, **2**, and (LH)₂L₂Cu₃I₄, respectively. This case study highlights the potential of combining octacyanidometalates and chiral building blocks and opens new perspectives in magnetochiral materials.

ASSOCIATED CONTENT

Supporting Information

Experimental data for (LH)₂L₂Cu₃I₄, ORTEP diagram of structural motifs of **1** and **2**, local environment of metal centers, hydrogen-bond network, SHAPE parameters for Cu^{II} and M^{IV} centers, diffuse reflectance solid-state UV–vis–NIR spectra of **1** and **2**, and results of photomagnetic studies. X-ray crystallographic information files (CIF) are available for compounds **1** and **2**. This material is available free of charge via the Internet at <http://pubs.acs.org>.

AUTHOR INFORMATION

Corresponding Author

*E-mail: barbara.sieklucka@uj.edu.pl

Author Contributions

The manuscript was written through contributions of all authors. All authors have given approval to the final version of the manuscript.

Notes

The authors declare no competing financial interest.

ACKNOWLEDGMENTS

We thank the Centre National de la Recherche Scientifique (CNRS), the Institut Universitaire de France (IUF), the Polish National Science Centre (Grant DEC-2011/01/B/ST5/00716), and the International PhD-studies Programme at the Faculty of Chemistry Jagiellonian University within the Foundation for Polish Science MPD Programme cofinanced by the EU European Regional Development Fund for financial support. The research was partially carried out with the equipment purchased thanks to the financial support of the European Regional Development Fund in the framework of the Polish Innovation Economy Operational Program (contract no. POIG.02.01.00-12-023/08).

DEDICATION

Dedicated to Professor Marius Andruh on the occasion of his 60th birthday.

REFERENCES

- (a) Komori-Orisaku, K.; Imoto, K.; Koide, Y.; Ohkoshi, S. *Cryst. Growth Des.* **2013**, *13*, 5267–5271. (b) Chorazy, S.; Podgajny, R.; Nitek, W.; Fic, T.; Görlich, E.; Rams, M.; Sieklucka, B. *Chem. Commun.* **2013**, *49*, 6731–6733. (c) Pinkowicz, D.; Rams, M.; Nitek, W.; Czarnecki, B.; Sieklucka, B. *Chem. Commun.* **2012**, *48*, 8323–8325. (d) Komori Orisaku, K.; Nakabayashi, K.; Ohkoshi, S. *Chem. Lett.* **2011**, *40*, 586–587. (e) Pinkowicz, D.; Podgajny, R.; Nitek, W.; Rams, M.; Majcher, A. M.; Nuida, T.; Ohkoshi, S.; Sieklucka, B. *Chem. Mater.* **2011**, *23*, 21–31. (f) Tsunobuchi, Y.; Kosaka, W.; Nuida, T.; Ohkoshi, S. *CrystEngComm* **2009**, *11*, 2051–2053. (g) Kosaka, W.; Hashimoto, K.; Ohkoshi, S. *Bull. Chem. Soc. Jpn.* **2008**, *81*, 992–994. (h) Higashikawa, H.; Okuda, K.; Kishine, J.; Masuhara, N.; Inoue, K. *Chem. Lett.* **2007**, *36*, 1022–1023. (i) Kosaka, W.; Nuida, T.; Hashimoto, K.; Ohkoshi, S. *Bull. Chem. Soc. Jpn.* **2007**, *80*, 960–962.
 - (a) Chorazy, S.; Nakabayashi, K.; Imoto, K.; Mlynarski, J.; Sieklucka, B.; Ohkoshi, S. *J. Am. Chem. Soc.* **2012**, *134*, 16151–16154. (b) Visinescu, D.; Jeon, I.-R.; Madalan, A. M.; Alexandru, M.-G.; Jurca, B.; Mathonière, C.; Clérac, R.; Andruh, M. *Dalton Trans.* **2012**, *41*, 13578–13581.
 - (a) Zhang, W.; Sun, H.-L.; Sato, O. *Dalton Trans.* **2011**, *40*, 2735–2743. (b) Koziel, M.; Podgajny, R.; Kania, R.; Lebris, R.; Mathonière, C.; Lewiński, K.; Kruczała, K.; Rams, M.; Labrugère, C.; Bousseksou, A.; Sieklucka, B. *Inorg. Chem.* **2010**, *49*, 2765–2772.

- (c) Zhang, W.; Sun, H.-L.; Sato, O. *Cryst. Eng. Commun.* **2010**, *12*, 4045–4047.
- (4) Chorazy, S.; Nakabayashi, K.; Ozaki, N.; Pelka, R.; Fic, T.; Mlynarski, J.; Sieklucka, B.; Ohkoshi, S. *RSC Adv.* **2013**, *3*, 1065–1068.
- (5) (a) Gogoi, N.; Thlijeni, M.; Duhayon, C.; Sutter, J.-P. *Inorg. Chem.* **2013**, *52*, 2283–2285. (b) Tong, Y.-Z.; Wang, Q.-L.; Su, C.-Y.; Ma, Y.; Ren, S.; Xu, G.-F.; Yang, G.-M.; Cheng, P.; Liao, D.-Z. *CrystEngComm* **2013**, *15*, 9906–9915. (c) Podgajny, R.; Korzeniak, T.; Przychodzeń, P.; Giménez-Saiz, C.; Rams, M.; Kwaśniak, M.; Sieklucka, B. *Eur. J. Inorg. Chem.* **2010**, *26*, 4166–4174. (d) Zhang, W.; Wang, Z.-Q.; Sato, O.; Xiong, R.-G. *Cryst. Growth Des.* **2009**, *9*, 2050–2053. (e) Korzeniak, T.; Desplanches, C.; Podgajny, R.; Giménez-Saiz, C.; Stadnicka, K.; Rams, M.; Sieklucka, B. *Inorg. Chem.* **2009**, *48*, 2865–2872. (f) Yuan, M.; Gao, S.; Zhao, F.; Zhang, W.; Wang, Z.-M. *Sci. China, Ser. B: Chem.* **2009**, *52*, 266–275. (g) Liu, W.-Y.; Zhou, H.; Guo, J.-X.; Yuan, A.-H. *Acta Crystallogr.* **2008**, *E64*, m1152–m1153. (h) Qu, J.; Gu, W.; Liu, X. J. *Coord. Chem.* **2008**, *61*, 1782–1787. (i) Purcell, W.; Visser, H. G. *Acta Crystallogr.* **2008**, *E64*, m1438–m1439. (j) Zhao, H.; Shatruck, M.; Prosvirin, A. V.; Dunbar, K. R. *Chem.—Eur. J.* **2007**, *13*, 6573–6589. (k) Przychodzeń, P.; Pelka, R.; Lewiński, K.; Supel, J.; Rams, M.; Tomala, K.; Sieklucka, B. *Inorg. Chem.* **2007**, *46*, 8924–8938. (l) Kosaka, W.; Hashimoto, K.; Ohkoshi, S. *Bull. Chem. Soc. Jpn.* **2007**, *80*, 2350–2356. (m) Withers, J. R.; Ruschmann, C.; Bojang, P.; Parkin, S.; Holmes, S. M. *Inorg. Chem.* **2005**, *44*, 352–358. (n) Korzeniak, T.; Stadnicka, K.; Rams, M.; Sieklucka, B. *Inorg. Chem.* **2004**, *43*, 4811–4813. (o) Kou, H.-Z.; Zhou, B. C.; Si, S.-F.; Wang, R.-J. *Eur. J. Inorg. Chem.* **2004**, 401–408. (p) Eckhardt, R.; Hanika-Heidl, H.; Fischer, R. D. *Chem.—Eur. J.* **2003**, *9*, 1795–1804. (q) Podgajny, R.; Korzeniak, T.; Stadnicka, K.; Dromzée, Y.; Alcock, N. W.; Errington, W.; Kruczala, K.; Balanda, M.; Kemp, T. J.; Verdaguer, M.; Sieklucka, B. *Dalton Trans.* **2003**, 3458–3468. (r) Chang, F.; Sun, H.-L.; Kou, H.-Z.; Gao, S. *Inorg. Chem. Commun.* **2002**, *5*, 660–663. (s) Li, D.-F.; Gao, S.; Zheng, L.-M.; Yu, K.-B.; Tang, W.-X. *New J. Chem.* **2002**, *26*, 1190–1195. (t) Sra, A. K.; Rombaut, G.; Lahitête, F.; Golhen, S.; Ouahab, L.; Mathonière, C.; Yakhmi, J. V.; Kahn, O. *New J. Chem.* **2000**, *24*, 871–876.
- (6) (a) Qian, S.-Y.; Zhou, H.; Yuan, A.-H.; Song, Y. *Cryst. Growth Des.* **2011**, *11*, 5676–5681. (b) Venkatakrishnan, T. S.; Sahoo, S.; Bréfuel, N.; Duhayon, C.; Paulsen, C.; Barra, A.-L.; Ramasesha, S.; Sutter, J.-P. *J. Am. Chem. Soc.* **2010**, *132*, 6047–6056. (c) Yoo, H. S.; Ko, H. H.; Ryu, D. W.; Lee, J. W.; Yoon, J. H.; Lee, W. R.; Kim, H. C.; Koh, E. K.; Hong, C. S. *Inorg. Chem.* **2009**, *48*, 5617–5619.
- (7) (a) Brossard, S.; Volatron, F.; Lisnard, L.; Arrio, M.-A.; Catala, L.; Mathonière, C.; Mallah, T.; Cartier dit Moulin, C.; Rogalev, A.; Wilhelm, F.; Smekhova, A.; Sainctavit, P. *J. Am. Chem. Soc.* **2012**, *134*, 222–228. (b) Ohkoshi, S.; Tokoro, H. *Acc. Chem. Res.* **2012**, *45*, 1749–1758. (c) Bleuzen, A.; Marvaud, V.; Mathonière, C.; Sieklucka, B.; Verdaguer, M. *Inorg. Chem.* **2009**, *48*, 3453–3466. (d) Brinzei, D.; Catala, L.; Mathonière, C.; Wernsdorfer, W.; Gloter, A.; Stephan, O.; Mallah, T. *J. Am. Chem. Soc.* **2007**, *129*, 3778–3779. (e) Ohkoshi, S.; Tokoro, H.; Hozumi, T.; Zhang, Y.; Hashimoto, K.; Mathonière, C.; Bord, I.; Rombaut, G.; Verelst, M.; Cartier dit Moulin, C.; Villain, F. *J. Am. Chem. Soc.* **2006**, *128*, 270–277. (f) Hozumi, T.; Hashimoto, K.; Ohkoshi, S. *J. Am. Chem. Soc.* **2005**, *127*, 3864–3869. (g) Herrera, J. M.; Marvaud, V.; Verdaguer, Marrot, J.; Kalisz, M.; Mathonière, C. *Angew. Chem., Int. Ed.* **2004**, *43*, 5468–5471.
- (8) (a) El Fallah, M. S.; Vicente, R.; Escuer, A.; Badyine, F.; Solans, X.; Font-Bardia, M. *Inorg. Chim. Acta* **2008**, *361*, 4065–4069. (b) El Fallah, M. S.; Badyine, F.; Vicente, R.; Escuer, A.; Solans, X.; Font-Bardia, M. *Dalton Trans.* **2006**, 2934–2942. (c) Wang, S. J. *Cluster Sci.* **1995**, *6*, 463–484.
- (9) (a) Chen, F.-T.; Li, D.-F.; Gao, S.; Wang, X.-Y.; Li, Y. Z.; Zhen, L. M.; Tang, W. X. *Dalton Trans.* **2003**, 3283–3287. (b) Wang, Z.-X.; Li, X.-L.; Liu, B.-L.; Tokoro, H.; Zhang, P.; Song, Y.; Ohkoshi, S.; Hashimoto, K.; You, X.-Z. *Dalton Trans.* **2008**, 2103–2106.
- (10) (a) El Fallah, M. S.; Badyine, F.; Vicente, R.; Escuer, A.; Solans, X.; Font-Bardia, M. *Chem. Commun.* **2006**, 3113–3115. (b) Elerman, Y.; Kavlakoglu, E.; Elmali, A.; Kendi, E. Z. *Naturforsch., B: J. Chem. Sci.* **2001**, *56*, 1123–1128. (c) Kivekas, R. *Finn. Chem. Lett.* **1978**, 58. (d) Nasakkala, M. *Ann. Acad. Sci. Fenn., Ser. A2* **1977**, 181, 6.
- (11) (a) Pajunen, A.; Kivekas, R. *Cryst. Struct. Commun.* **1979**, *8*, 385–391. (b) Bertrand, J. A.; Marabella, C. P.; Vanderveer, D. G. *Inorg. Chim. Acta* **1977**, *25*, L69–L70. (c) Kivekas, R.; Pajunen, A.; Smolander, K. *Finn. Chem. Lett.* **1977**, 256.
- (12) (a) Szklarzewicz, J.; Matoga, D.; Lewiński, K. *Inorg. Chim. Acta* **2007**, *360*, 2002–2008. (b) Matoga, D.; Szklarzewicz, J.; Mikurya, M. *Inorg. Chem.* **2006**, *45*, 7100–7104.
- (13) (a) Farrugia, L. J. *J. Appl. Crystallogr.* **1999**, *32*, 837–838. (b) Altomare, A.; Burla, M. C.; Camalli, M.; Cascarano, G. L.; Giacovazzo, C.; Guagliardi, A.; Moliterni, A. G. G.; Polidori, G.; Spagna, R. *J. Appl. Crystallogr.* **1999**, *32*, 115–119. (c) Sheldrick, G. M. *Acta Crystallogr.* **2008**, *A64*, 112–122. (d) Orpen, A. G. *J. Chem. Soc., Dalton Trans.* **1980**, 2509–2516. (e) Macrae, C. F.; Bruno, I. J.; Chisholm, J. A.; Edgington, P. R.; McCabe, P.; Pidcock, E.; Rodriguez-Monge, L.; Taylor, R.; van de Streek, J.; Wood, P. A. *J. Appl. Crystallogr.* **2008**, *41*, 466–470. (f) Llunell, M.; Casanova, D.; Cirera, J.; Alemany, M. P.; Alvarez, S. *SHAPE*, v.2.0; Universitat de Barcelona: Barcelona, 2010.
- (14) Zheng, X.-D.; Jiang, L.; Feng, X.-L.; Lu, T.-B. *Dalton Trans.* **2009**, 6802–6808.
- (15) (a) Pilawa, B.; Schuhmacher, J. J. *Phys.: Condens. Matter* **1996**, *8*, 1539–1555. (b) Kahn, O. *Molecular Magnetism*; VCH: New York, 1993; Chapters 1 (1.5), 10 (10.2).